 https://doi.org/10.3311/PPci.19683

Periodica Polytechnica Civil Engineering, 67(1), pp. 24–35, 2023

Numerical Investigation of the Effects of Ground Motion Characteristics on the Seismic Behavior of Liquefiable Soil

Selçuk Demir[1*]

[1] Department of Civil Engineering, Engineering Faculty, Bolu Abant Izzet Baysal University, 14030, Bolu, Turkey
[*] Corresponding author, e-mail: selcukdemir@ibu.edu.tr

Received: 10 December 2021, Accepted: 19 September 2022, Published online: 21 September 2022

Abstract

The seismic behavior of liquefiable soils can be significantly influenced by many ground motion characteristics. Therefore, it is crucial to identify the ground motion characteristics that have the most significant effects on the seismic behavior of liquefiable soils. In this paper, a series of nonlinear numerical analyses were performed to investigate the influence of ground motion characteristics on the seismic behavior of loose liquefiable soil. The liquefiable soil profiles were built with the same relative densities but different layer thicknesses. In order to clarify the effect of the ground motion characteristics on the liquefiable soil mechanism, soil profiles were subjected to ground motion sets having different characteristics, such as maximum horizontal accelerations, frequency contents, and significant durations. The numerical analyses were performed using the open-source program OpenSees. The results were presented and discussed in terms of peak ground acceleration, amplification ratio, maximum excess pore pressure ratio, maximum shear strain, and maximum lateral displacement. The results indicated that the maximum horizontal acceleration and the frequency content greatly influence the site response behavior of the liquefiable soil. Furthermore, the nonlinear behavior of the soil is more obvious on being subjected to long-duration ground motions as compared to shorter duration ground motions having the same maximum horizontal acceleration. The findings presented in this study could be helpful when analyzing the seismic response of liquefiable soils coupling superstructures.

Keywords

ground motion characteristics, liquefaction, numerical analyses, opensees

1 Introduction

Earthquakes are one of the natural hazards that have caused significant damage to structures, lifelines, and great loss of human life. Earthquake-induced seismic waves at a site propagate through different geological formations until they reach the ground surface. Observations from earthquakes such as 1964 Niigata (Japan) and Alaska (USA), 1976 Tangshan (China), 1999 Kocaeli (Turkey), 2011 Tohoku (Japan), and the 2010-2011 Christchurch (New Zealand) earthquakes showed that many cases of structural damage or ground failure are caused by soil liquefaction [1–7]. Thus, the site effect of the propagated seismic waves through liquefiable soil profiles on existing or new structures is a crucial issue in geotechnical or geological engineering for a proper understanding of seismic hazards.

Some previous case studies have investigated the seismic behavior of liquefiable soils during earthquake shaking and provided useful insights [8–12]. These works confirmed that coupled nonlinear numerical analysis should be used for seismic design due to modification of ground surface motions during the generation of excess pore water pressure. Youd and Carter [11] and Gingery et al. [13] investigated the behavior between soil liquefaction and spectral accelerations using ground motions at liquefaction sites. They have shown that the characteristics of ground shaking significantly alter due to soil liquefaction. They have also reported that soil liquefaction tends to amplify longer-period spectral accelerations, while the spectral accelerations often decrease in amplitude for shorter periods. On the other hand, a limited number of researchers have used shaking table and centrifuge tests to understand the seismic behavior of liquefiable soils and their effects on the ground surface [14–16]. For instance, Su et al. [15] performed an experimental study on saturated sand models to study the effect of maximum horizontal accelerations

Cite this article as: Demir, S. "Numerical Investigation of the Effects of Ground Motion Characteristics on the Seismic Behavior of Liquefiable Soil", Periodica Polytechnica Civil Engineering, 67(1), pp. 24–35, 2023. https://doi.org/10.3311/PPci.19683

(shaking strength) on the behavior of liquefied sand during earthquake excitation. Vertical and horizontal displacements, acceleration, and excess pore water pressure measurements were recorded in the experiment to interpret test results. Their results indicated that maximum horizontal acceleration has a pronounced effect on excess pore pressure buildup, displacements, and amplification ratio. Adampira et al. [16] conducted a series of shaking table tests to evaluate the seismic response of the soil profile having liquefiable sub-layers. The results demonstrated that the liquefiable sub-layers could alter the main characteristics of the seismic site response, primarily depending on the level of excess pore water pressure and soil softening in the layer.

Numerical analyses are another key tool for understanding the site effects of liquefiable soils due to the propagation of ground motion during an earthquake shaking [17]. Many previous studies have performed nonlinear effective stress numerical studies using hypothetical liquefiable soil profiles [18–20]. In these studies, researchers mainly focused on the relationship between excess pore water pressures with amplitudes and frequency contents of the ground motions. Similarly, various investigators have numerically modeled case study examples and investigated the nonlinear behavior of liquefiable soils [21, 22]. In these studies, researchers have discussed the effect of excess pore pressure generation on acceleration time histories, as well as response spectra at the ground surface.

Bouckovalas et al. [23] examined seismic recordings obtained from the Port Island downhole array and the Wild-life Liquefaction Array, during the Kobe and the Superstition Hills earthquakes. Also, they performed analytical and numerical work on the non-liquefied crust overlying liquefied sand profile to investigate the seismic response of the layered liquefiable soil. From field case studies and numerical analyses, they concluded that liquefied soil layers could attenuate or amplify the ground motion relying on the liquefied layer thickness and the seismic excitation period. Accordingly, Adampira and Derakhshandi [24] performed nonlinear parametric analyses on the layered liquefiable soil profiles and examined the influence of maximum horizontal acceleration, liquefiable sublayer thickness, and liquefiable sub-layer depth on the seismic behavior of the soil profiles during shaking. They reported that liquefiable sub-layers played a vital role on the intensity of seismic waves and earthquake-induced forces. Similar conclusions with regard to the amplification or attenuation effects of a layered liquefied soil profile were also drawn from Adampira et al. [25].

Considering the studies mentioned above, there are still unknown aspects of the seismic behavior of the liquefiable soils. It should be noted that these studies generally have focused on site response behavior of the layered liquefiable soils by taking into account excess pore water pressure generation, acceleration-time history, or response spectra. More detailed numerical studies on the simple liquefiable soil profiles would be beneficial for a better understanding of simple or multi-layered liquefiable soil profiles. This paper aims to investigate the seismic behavior of liquefiable soils considering different ground motion characteristics. For this purpose, a homogeneous soil profile comprised of loose sand was utilized during the numerical analyses to represent the liquefiable soil. Nonlinear effective stress site response analyses were performed to explore the influence of the maximum horizontal acceleration (a_{max}), the frequency content (f_p), and significant durations ($D_{5–95\%}$) of the earthquake records on the liquefiable soil behavior using the OpenSees platform. Moreover, the influence of various soil layer thicknesses on the response of the liquefiable soil profile was also considered. The seismic site response behavior of liquefiable soils during earthquake shaking was discussed elaborately in terms of peak ground acceleration (*PGA*), amplification ratio (A_R), maximum excess pore pressure ratio ($r_{u,max}$), maximum shear strain (γ_{max}), and maximum lateral displacement (Ld_{max}).

2 Numerical modeling

A soil column comprised of a homogeneous liquefiable soil with variable thicknesses (H) was used in numerical simulations, as shown in Fig. 1. The soil profile was built with loose sand with a relative density (D_r) of 40%. The groundwater table (*GWT*) was located at the ground surface.

The soil profile was discretized in sublayers based on the rule proposed by [26] in order to allow an appropriate wave propagation in the soil profile. This rule suggests that

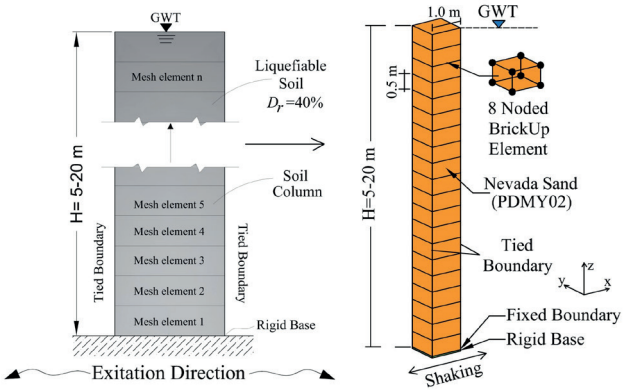

Fig. 1 Element discretization and other details of the OpenSees model

the element size (h_{max}) after meshing should be $h_{max} \leq 1/(8–10)\lambda_{min}$ (λ_{min}: the minimum wavelength). The maximum mesh sizes used in simulations were set to 1.0 m and 0.5 m in horizontal and vertical directions, respectively. The bottom of the model was fixed in both horizontal and vertical directions and formed as a rigid base to provide ground motion from this layer. Nodes at the same location on the lateral boundaries were tied to have equal displacements in the X direction and free to move in the Z direction.

Soil layers were built up using eight-node BrickUP element based on the *u–p* formulation [27] to simulate fully coupled soil response. Each node has three degrees of freedom (DOF) for translational displacements (*u*) of a soil skeleton and one DOF for pore water pressure (*p*). An advanced constitutive model, Pressure Dependent Multi Yield02 (PDMY02) [28], was used in this study to represent the nonlinear monotonic or cyclic response of the soil under drained or undrained conditions. This model is an elastoplastic model based on the multi-yield-surface-plasticity theory [29]. The model uses a non-associative rule to define the dilative or contractive behavior of soils.

The PDMY02 model parameters used in this study (Table 1) are selected based on calibrated values for the liquefiable Nevada sand (D_r = 40%) by Demir [30], including octahedral shear modulus of the soil ($G_{max,oct}$), bulk modulus of the soil (B_r), maximum octahedral shear strain ($\gamma_{max,r}$), cohesion (c), triaxial friction angle (ϕ°_{txc}) phase transformation angle (ϕ°_{pt}), number of yield surface (*NYS*), contraction (c_1, c_2, c_3), and dilation parameters (d_1, d_2, d_3).

Moreover, in this study, the ability of the calibrated model parameters given in Table 1 for predicting typical element level monotonic and cyclic behavior of the liquefiable soil was also investigated and numerical results were compared with the laboratory test measurements performed by Arulmoli et al. [31] (Fig. 2 and Fig. 3). It is seen that a reasonable match with the experimental study under different effective confinement pressures (40, 80, and 160 kPa) was achieved using calibrated parameters for drained monotonic triaxial compression test. Also, the simulation capability of the model under undrained cyclic direct simple shear test (CDSS) generally captured the cyclic behavior of the measured data to an acceptable degree.

Table 1 PDMY02 model parameters [30]

Parameter	Description	Value
ρ (ton/m^3)	Density	1.96
p_{ref} (kPa)	Reference effective confining stress	100
$G_{max,oct}$ (MPa)	Octahedral low-strain shear modulus	50
$\gamma_{max,r}$ (%)	Maximum octahedral shear strain	0.1
B_r (MPa)	Bulk modulus	122
d	Pressure dependency coefficient	0.5
c (kPa)	Cohesion	0.1
ϕ°_{txc}	Triaxial friction angle	32
ϕ°_{pt}	Phase transformation angle	27
c_1, c_2, c_3	Contraction and dilation coefficients	0.025, 4.5, 0.2
d_1, d_2, d_3		0.1, 3.0, 0.0
NYS	Number of yield surface	20

3 Ground motion characteristics

Ground motions contain a tremendous amount of information. Thus, identifying a ground motion may be complicated. There are various characteristics to express a ground motion. However, ground motions are characterized by their maximum horizontal acceleration, frequency content, and duration of the motion for engineering purposes [32]. In this study, different records were chosen in the numerical simulations covering a wide range of maximum horizontal accelerations, predominant frequencies, and significant durations. Details of ground motion characteristics and records used in numerical analyses are provided as follows.

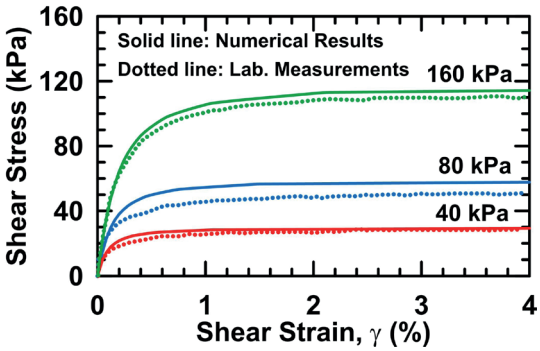

Fig. 2 Comparison of measured and simulated drained monotonic triaxial compression test results for D_r = 40%

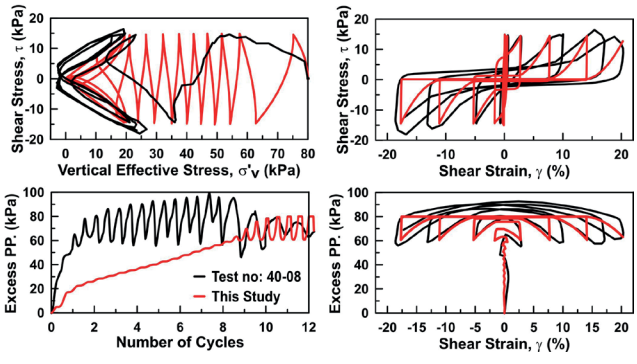

Fig. 3 Comparison of measured and simulated CDSS results (Test No: 40-08, CSR = 0.181, σ_v' = 80 kPa)

3.1 Maximum horizontal acceleration (a_{max})

In order to investigate the effect of maximum horizontal accelerations on the seismic behavior of the liquefiable soil, the soil profile was excited by the scaled versions of a ground motion given in Fig. 4. The ground motion was scaled to a_{max} = 0.05 g, 0.1 g, 0.2 g, 0.4 g and 0.8 g for representing weak-to-strong input motion intensities with applying the same frequency content.

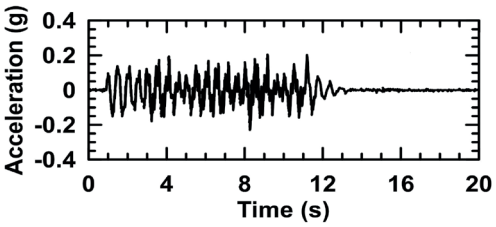

Fig. 4 A sample of acceleration time history used for maximum horizontal acceleration simulations

3.2 Frequency content (f_p)

In this study, the predominant frequency (f_p) was selected to define the frequency content of a ground motion and investigate its influence on liquefiable soil behavior. Nonlinear effective stress analyses were conducted considering a group of five ground motions with different f_p values. For this, the soil profile was subjected to real earthquake excitations, namely Imperial Valley (*IV*), Loma Prieta (*LP*), Düzce (*DZ*), Coyote Lake (*CL*), and Cape Mendocino (*CM*). All input motions were linearly scaled to maximum horizontal acceleration a_{max} of 0.20 g. Details of these input motions are described in Table 2. The acceleration-time histories and corresponding Fourier amplitudes of the selected input motions are given in Fig. 5.

Table 2 Some characteristics of the input motions used in frequency content simulations

Earthquake	ID	Record No	I_a (m/s)	f_p (Hz)
Imperial Valley, 1979	IV	HVP-315	1.57	0.29
Loma Prieta, 1989	LP	HCH-090	1.21	1.10
Duzce, 1999	DZ	DZC-180	2.01	2.32
Coyote Lake, 1979	CL	G02-050	0.59	4.83
Cape Mendocino, 1992	CM	SLH-090	1.14	7.22

3.3 Significant duration ($D_{5–95\%}$)

$D_{5–95\%}$ can be explained as the time interval at which a specified amount of energy is dissipated (5 and 95% of the Arias intensity (I_a) of the ground motion). The I_a value measures the acceleration of transient seismic waves to determine the intensity of shaking. Selection of the candidate $D_{5–95\%}$

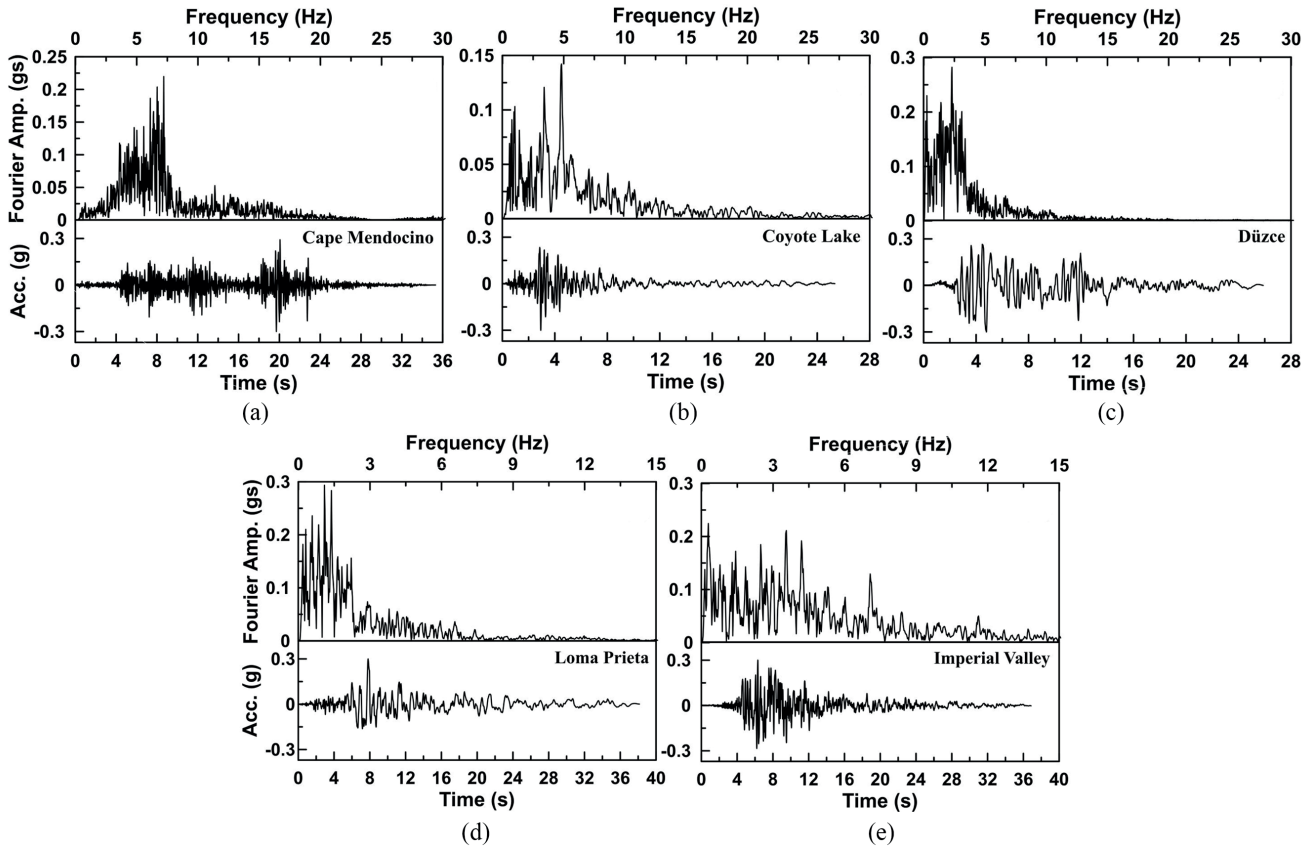

Fig. 5 Acceleration time histories and Fourier amplitudes of the earthquake motions (a) CM, (b) CL, (c) DZ, (d) LP, and (e) IV

values was made from the Chi-Chi (Taiwan) earthquake. Fig. 6 illustrates acceleration and Arias intensity time history records of the selected motions. A significant duration range of $D_{5–95\%}$ = 5.8–80.9 s was used during simulations. Also, all records were scaled to a constant acceleration of a_{max} = 0.20 g to provide maximum acceleration consistency. The list of the selected Chi-Chi earthquake records and the relevant information is given in Table 3.

Table 3 Chi-Chi earthquake records used in the study

Record No	I_a (m/s)	a_{max} (g)	f_p (Hz)	$D_{5–95\%}$ (s)
CHY028	0.35	0.2	1.18	5.8
TCU045	0.18	0.2	1.32	10.8
TCU128	1.14	0.2	0.26	20.7
CHY044	2.72	0.2	0.28	40.0
CHY094	3.70	0.2	0.15	80.9

4 Results

In this section, the effects of ground motion characteristics, such as maximum horizontal acceleration, frequency content, and significant duration on the seismic soil behavior were evaluated in terms of *PGA*, A_R, r_u, γ_{max}, and Ld_{max}. Moreover, numerical analyses were performed considering variable soil layer thicknesses. The thickness (H) of the liquefiable soil layer was considered in order of 5, 7, 10, 15, and 20 m during simulations.

4.1 Effect of a_{max} values

4.1.1 Response of peak ground accelerations (*PGA*)

Fig. 7 presents the variation of peak ground accelerations (*PGA*) throughout the soil profile with different maximum horizontal accelerations for the layer thickness of H = 10 m. It is seen that from Fig. 7, the *PGA* values in the liquefiable soil are significantly influenced by the a_{max} values. An increase in a_{max} from 0.05 g to 0.2 g led to an increase in *PGA* values. However, *PGA* values decreased when a_{max} exceeded 0.2 g. When the soil was shaken under strong a_{max} values, the soil tended to undergo significant attenuation due to the isolation effect of the soil liquefaction [33].

In order to clearly demonstrate the effect of a_{max} on the *PGA* values, soil profiles having different layer thicknesses were shaken, and results were presented in terms of *PGA* and amplification ratio (A_R). A_R is the ratio of the maximum horizontal acceleration of the soil surface to the acceleration of base ground motion. Fig. 8 shows an example of the effect of amax on the developed peak ground accelerations and amplification ratios with the variation of the thickness of the soil layer. In general, the trend for the relationship shows that increasing a_{max} increases the *PGA* values for all layer thicknesses used in the analyses. On the other hand, while the increase of the liquefiable layer thickness leads to a slight change in *PGA* values for $a_{max} \leq 0.2$ g, the effect of H values is more evident on the *PGA* value for $a_{max} > 0.2$ g. It can be concluded that from Fig. 8(a), accelerations transferred to the ground

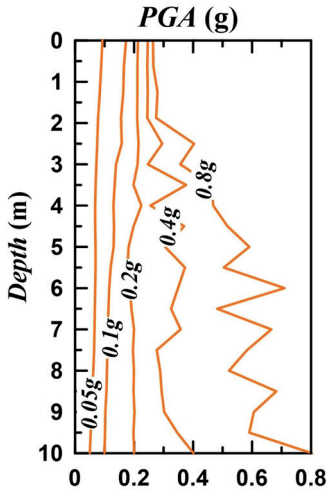

Fig. 7 Variation of PGA with a_{max} for H = 10 m

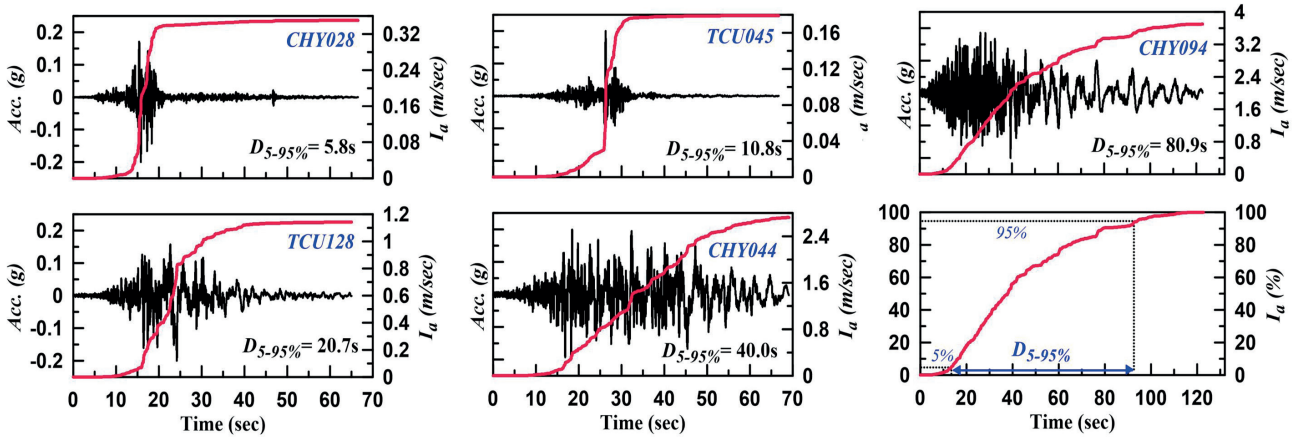

Fig. 6 Acceleration time histories of Chi-Chi earthquake records

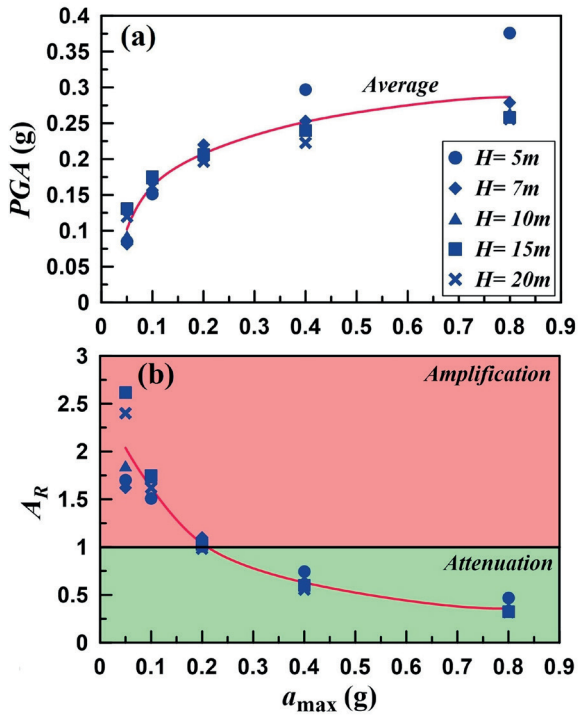

Fig. 8 Change of *PGA* and A_R with a_{max} for different layer thicknesses (a and b)

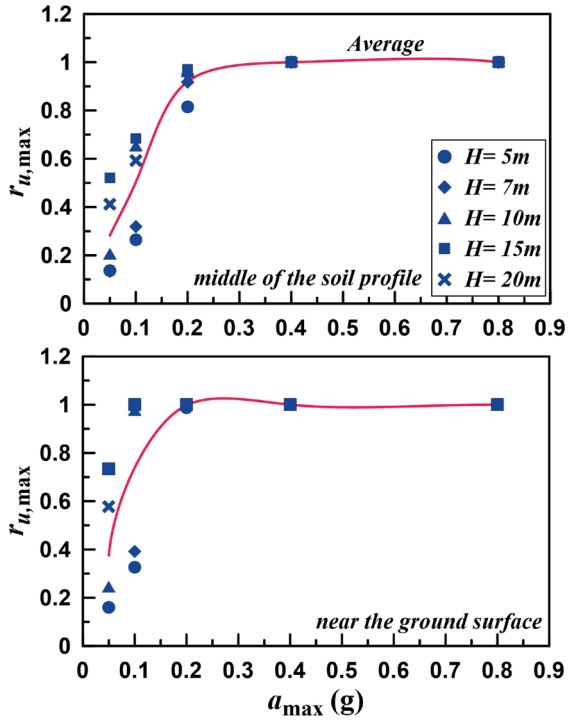

Fig. 9 Simulation results of $r_{u,max}$ at different depths for different a_{max} and H values

surface were reduced as the thickness of the liquefiable soil layer increased. Similar conclusions for the H vs PGA relationship were reported by Bouckovalas et al. [23] and Adampira and Derakhshandi [24] for multi-layered liquefiable soils.

During the weak-to-medium intensities (a_{max} = 0.05 g and 0.1 g), accelerations were completely amplified over the entire layer thickness range (Fig. 8(b)). It is also observed that an increase in the a_{max} value leads to an attenuation of accelerations (A_R < 1.0), especially for a_{max} higher than 0.2 g. The results imply that maximum horizontal accelerations and liquefiable layer thickness have an important role on the amplification or de-amplification behavior of the liquefiable soil.

4.1.2 Response of maximum excess pore water pressure ratios ($r_{u,max}$)

Due to seismic loading, excess pore water pressures can be developed at loose soil deposits. Variation of maximum excess pore water pressure ratios ($r_u = \Delta u/\sigma'_{v0}$) with respect to a_{max} and H at two different depths are presented in Fig. 9. As it is illustrated in Fig. 9, the susceptibility of the soil to liquefaction increases as the a_{max} increase from a value of 0.05–0.2 g. However, for larger values of a_{max}(a_{max} ≥ 0.2 g), the excess pore water pressure ratios fluctuate around 1.0 that indicating liquefaction in the soil profile for both depths. Nonetheless, the $r_{u,max}$ is not significantly influenced by the change in thickness of the liquefiable layer when a_{max} exceeds 0.2 g. The $r_{u,max}$ values generally increase as a consequence of the increase in the value of layer thicknesses for a_{max} < 0.2 g, meaning that soil layers having higher thickness have higher excess pore pressures.

4.1.3 Response of shear strains (γ_{max}) and lateral displacements (Ld_{max})

The curves in Fig. 10 show the maximum shear strain and maximum lateral displacement distribution of the soil profile under weak-to-strong acceleration intensities. It is noticeably seen from Fig. 10(a) that the increase of a_{max} leads to an increase in the shear strain level of the soil. For instance, when a_{max} increases from 0.05 g to 0.8 g, the maximum shear strain on the soil profile reaches from 0.035% to 4%. This is expected because liquefiable soils exhibit nonlinear behavior when soil layers are subjected to strong motions, which leads to the development of large shear strains in soil. Inspecting Fig. 10(a) also reveals that the soil shear strains for the lower H values are usually lower than those at the higher thicknesses during a_{max} < 0.2 g. On the contrary, thinner soil layers are exposed to more shear strains than the thicker ones at higher acceleration levels (i.e., a_{max} = 0.8 g).

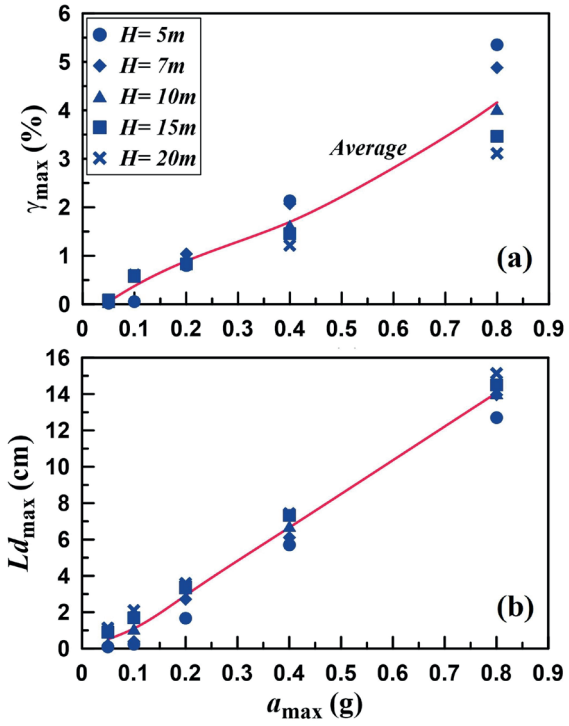

Fig. 10 Simulation results of (a) maximum shear strains and (b) lateral displacements for different a_{max} and H values

Fig. 10(b) shows that maximum lateral displacements at the ground surface follow a similar trend to that of the maximum shear strains observed on the soil profile. As expected, the values of Ld_{max} linearly increase with the increase in a_{max} and H values. This can be explained by the reduction of the soil strength and stiffness of the soil that occurs when the earthquake acceleration increases.

4.2 Effect of f_p values

4.2.1 Response of peak ground accelerations (*PGA*)

Fig. 11 shows the variation of *PGA* values in the liquefiable soil layer (H = 10 m) computed during different earthquake loadings. It is observed from Fig. 11 that the change in f_p has little influence on the *PGA* distributions. For all numerical analyses, *PGA* values in the soil slightly change through the soil profile.

Fig. 12(a) and (b) displays the variation of *PGA* and A_R values with respect to predominant frequency and layer thickness, respectively. Fig. 12 indicates that increasing the frequency content of the ground motion from 0.29 Hz to 7.22 Hz does not noticeably influence the resulting peak ground accelerations and amplification ratios. A_R values oscillate around 1.0 as f_p increases during numerical simulations. Similarly, the change of *PGA* and A_R values with the increment of layer thicknesses is not pronounced. In general, numerical predictions exhibit minor acceleration discrepancies at thicknesses between 5 and 20 m.

4.2.2 Response of maximum excess pore water pressure ratios ($r_{u,max}$)

The excess pore pressures developed in a saturated soil layer can be significantly influenced by the frequency content of a ground motion [34]. The maximum excess pore water pressure ratios in the soil with varying frequency content and layer thickness are presented in Fig. 13. Larger $r_{u,max}$ values are predicted when using ground motions that have lower frequency content. The maximum excess pore water pressure during *IV*, *LP*, and *DZ* motions reaches nearly each respective initial vertical effective stress (r_u = 0.8–1.0) near the ground surface. However, the soil

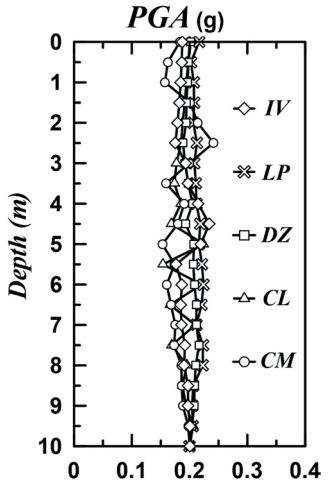

Fig. 11 Variation of *PGA* with f_p for H = 10 m

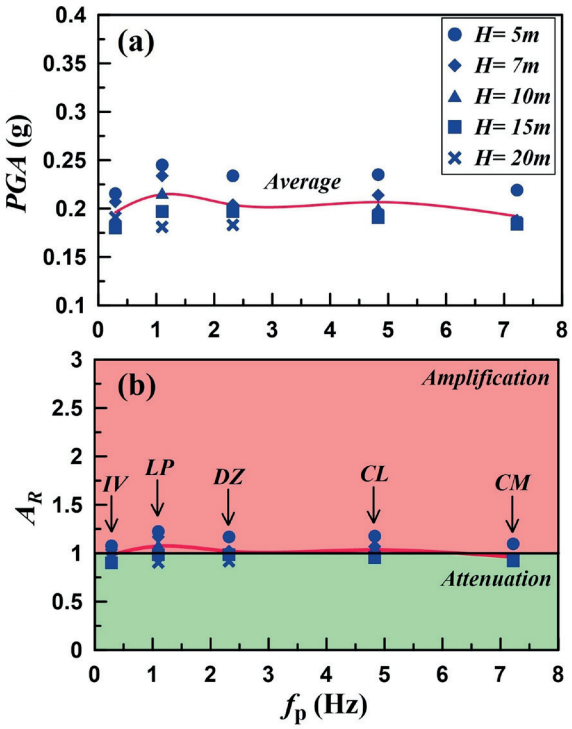

Fig. 12 Change of *PGA* and A_R with f_p for different layer thicknesses (a and b)

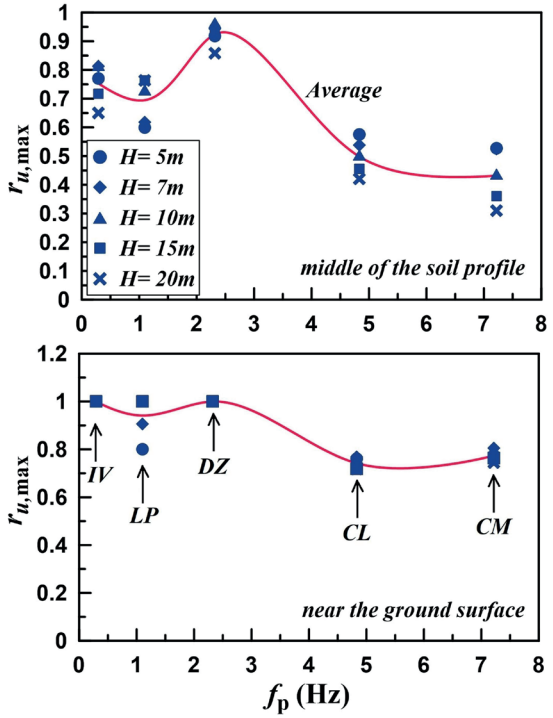

Fig. 13 Simulation results of $r_{u,max}$ at different depths for different f_p and H values

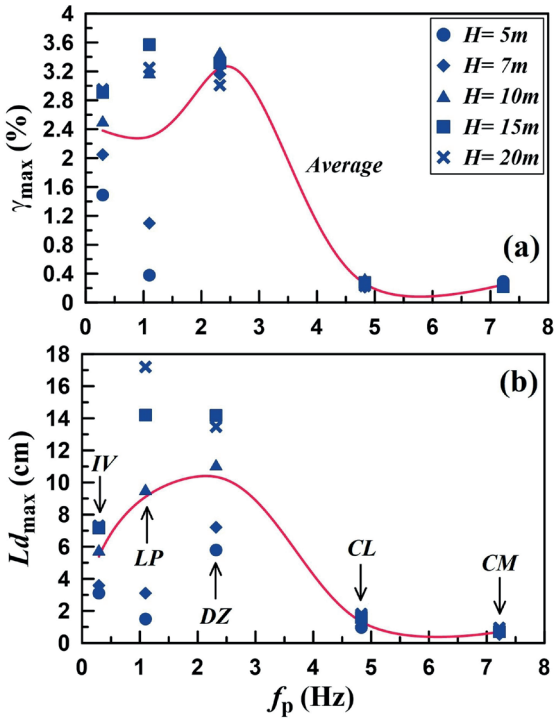

Fig. 14 Simulation results of (a) maximum shear strains and (b) lateral displacements for different f_p and H values

profile does not reach the liquefaction state ($r_u < 0.8$) under *CL* and *CM* motions in the case of higher f_p values. This is due to the predominant frequency of the ground motion. As it is known, the soil stiffness decreases during liquefaction and the fundamental frequency of the soil profile shifts to lower values [35, 36]. Therefore, the soil becomes more sensitive to seismic loading when its fundamental frequency is closer to the predominant frequency of the earthquake motion. Also, while $r_{u,max}$ values decrease as the layer thickness increases at the middle of the soil profile, variations in H have no serious effects on the $r_{u,max}$ values near the ground surface.

4.2.3 Response of maximum shear strains (γ_{max}) and lateral displacements (Ld_{max})

Maximum shear strain and maximum lateral displacement behavior of the soil under different frequency content and layer thickness are shown in Fig. 14(a) and Fig. 14(b), respectively. It is clear that the frequency content of input motions significantly influences the shear strain and lateral displacement response of the liquefiable soil. In accordance with the results above, generally larger shear strains are predicted throughout the soil profile when using input motions with lower frequency content. When the soil is subjected to ground motions with the lower predominant frequency, the accumulation of shear strain is more and therefore, larger lateral displacements are observed at the ground surface (Fig. 14(b)). Lateral displacements are relatively high during *IV*, *LP*, and *DZ* motions, reaching the maximum 17 cm for H = 20 m. However, it is only about 1.0–2.0 cm for the same layer thickness during *CL* and *CM* motions. As discussed above, this is related to the reduction of stiffness and soil softening during ground motions with lower frequency content. It should also be noted that when the liquefiable layer thickness is increased, larger lateral shear strains and lateral displacements are obs
erved during low-frequency contents ($f_p \leq 2.32$ Hz). For instance, the values of γ_{max} and Ld_{max} increased by approximately 98% and 135% as the thickness of the liquefiable layer increased from 5 m to 20 m during the *IV* motion.

4.3 Effect of $D_{5–95\%}$ values

4.3.1 Response of peak ground accelerations (*PGA*)

It is well-known that ground motion duration may strongly influence on liquefaction-induced earthquake damages [30]. For this, Fig. 15 explicates the peak ground acceleration-significant duration ($PGA–D_{5–95\%}$) relationship obtained from numerical simulations for H = 10 m. The *PGA* values initially increase with increasing $D_{5–95\%}$, however, *PGA* decreases as $D_{5–95\%}$ increase after the value of $D_{5–95\%}$ = 20.7 s between 0–4 m depths. On the other hand, there is essentially no distinct trend between *PGA* and $D_{5–95\%}$

at depths lower than 4.0 m. In order to give a more clear picture of the effect of significant duration on *PGA* and A_R variations, numerical analysis results are plotted in Fig. 16(a) and Fig. 16(b) for the soil profiles with the different layers thicknesses. According to the results shown in Fig. 16, as previously described in Fig. 15 for H = 10 m, increasing the significant duration of the ground motion rises *PGA* values at the ground surface for all given layer thicknesses for durations between 5.8 s and 20.7 s, and hence, there is a slight amplification (A_R > 1.0) at these durations. Moreover, long significant durations (i.e., 40 s and 80.9 s) increase the nonlinear effects on the seismic response of liquefiable soil, such as the cyclic degradation that produces soil strength and stiffness decrease. Therefore, *PGA* values tend to undergo an attenuation as duration increases in the case of $D_{5–95\%}$ > 20.7 s. Also, the *PGA* variation is significantly influenced by layer thickness during long $D_{5–95\%}$ values, and thinner soil profiles are exposed to higher *PGA* values if compared with thicker ones.

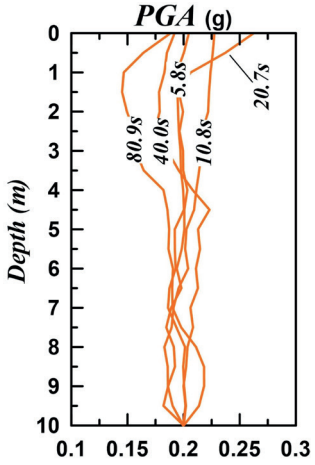

Fig. 15 Variation of *PGA* with $D_{5–95\%}$ for H = 10 m

4.3.2 Response of maximum excess pore water pressure ratios ($r_{u,max}$)

Fig. 17 presents the influence of $D_{5–95\%}$ and layer thickness on $r_{u,max}$ for two depths. In general, the thickness of the soil profile does not significantly affect the excess pore water pressure ratios. The discrepancy of $r_{u,max}$ values for different layer thicknesses is not pronounced at two depths. Additionally, $r_{u,max}$ is observed to be reached $r_{u,max}$ = 1.0 except for $D_{5–95\%}$ = 10.8 s during significant durations near the ground surface, which indicates the occurrence of liquefaction in the soil profile. This may be due to the imposed energy of the ground motion (*TCU045*) to the liquefiable soil profile, which has lower arias intensity as compared to the other motions. A similar trend is seen from Fig. 17 at the middle depth of the soil profile that while $r_{u,max}$ oscillates around 0.4–0.7 during numerical simulations for $D_{5–95\%} \leq$ 10.8 s, it achieves nearly 1.0 in the case of $D_{5–95\%}$ > 10.8 s.

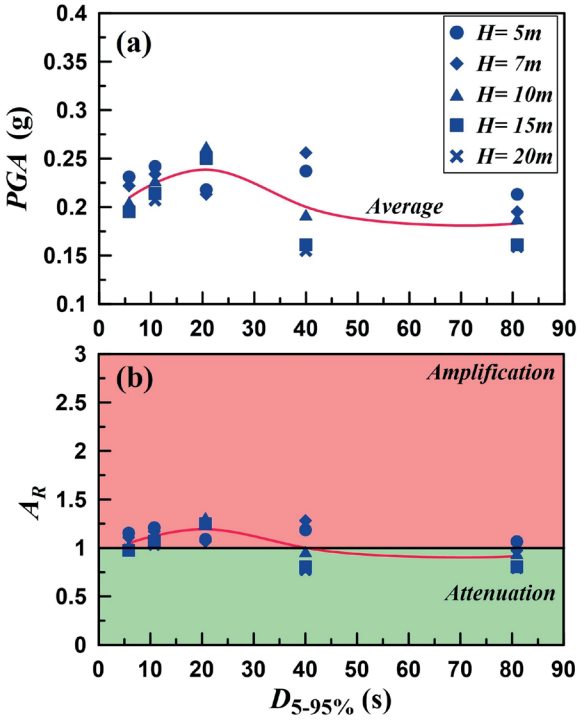

Fig. 16 Change of *PGA* and A_R with $D_{5–95\%}$ for different layer thicknesses (a and b)

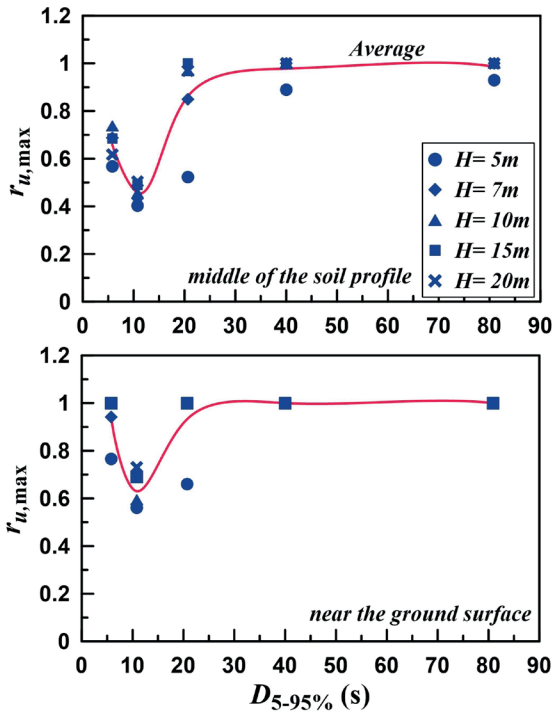

Fig. 17 Simulation results of $r_{u,max}$ at different depths for different $D_{5–95\%}$ and H values

4.3.3 Response of maximum shear strains (γ_{max}) and lateral displacements (Ld_{max})

Finally, the effect of significant duration is analyzed in Fig. 18 in terms of maximum shear strains and maximum lateral displacements. The nonlinear effects are seen to be more obvious for long significant durations since the shear strains and lateral displacements caused by the large duration motions such as *CHY044* (40.0 s) and *CHY094* (80.9 s) events are higher than the ones caused by small duration motion such as *CHY028* (5.8 s) and *TCU045* (10.8 s) events. γ_{max} and Ld_{max} increases become more evident as significant duration increases. Thus, γ_{max} and Ld_{max} drastically increase after the significant duration of 10.8 s and reach the maximum value of approximately 13% ($D_{5–95\%}$ = 80.9 s, H = 10 m) and 65 cm ($D_{5–95\%}$ = 40 s, H = 20 m), respectively. As explained above, this is due to the stiffness and strength behavior of the soil. The longer $D_{5–95\%}$ values cause to undergo of the soil a larger number of load reversal cycles and then softening, resulting in a higher accumulation of shear strains and lateral displacements at higher levels of significant durations even for maximum acceleration level of ground motions of 0.2 g. Remarkably, the maximum lateral displacements (Fig. 18(b)) at the ground surface increase as layer thickness increases. The Ld_{max} in the H = 20 m condition is about 5.0 times greater than that in the H = 5 m condition.

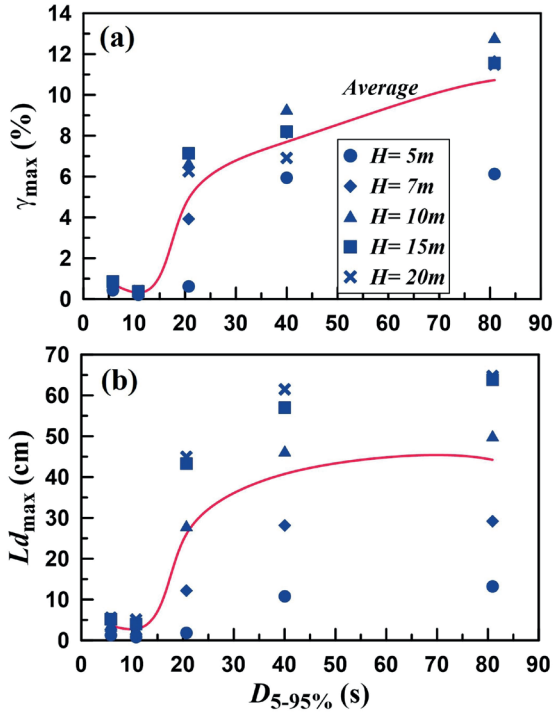

Fig. 18 Simulation results of (a) maximum shear strains and (b) lateral displacements for different $D_{5–95\%}$ and H values

5 Conclusions

The influence of ground motion characteristics on the seismic behavior of liquefiable soils with different thicknesses was studied in this paper. To this end, a homogenous liquefiable soil profile was modeled in the OpenSees platform. Based on the numerical analyses performed, the main conclusions of this study are:

- The increase in maximum horizontal accelerations (a_{max}) increases peak ground accelerations (PGA), shear strains (γ_{max}), and lateral displacements (Ld_{max}) for all layer thicknesses (H). On the other hand, a threshold acceleration of a_{max} = 0.2 g totally changes the seismic behavior of the soil in terms of amplification ratio (A_R) and excess pore pressure ratio (r_u). When the threshold acceleration is exceeded, the soil profile is totally liquefied (r_u = 1.0), and accelerations at the ground surface are attenuated (A_R < 1.0). More clearly, for events under strong input motion intensities (e.g., $a_{max} \geq 0.2$ g), soil behaves nonlinearly, inducing considerable modulus reduction and damping ratio increase as well as the large energy consumption with the propagation. Thus, the high frequency component attenuates rapidly and results in de-amplification of a_{max}.
- Despite the slight influence of the frequency content (f_p) on PGA and A_R, the f_p value plays an important role in the overall behavior of the liquefiable soil in the case of r_u, γ_{max}, and Ld_{max}. Larger r_u values are predicted when using ground motions that have lower frequency content. In accordance with the results of r_u, larger γ_{max} and Ld_{max} are predicted during earthquakes with low-frequency contents due to the increase of soil nonlinearity and damping. In addition, the quantity of γ_{max} and Ld_{max} are considerably increasing as H increases.
- Using the longer significant duration ($D_{5–95\%}$) brings an attenuation of PGA values as well as an increase of r_u and γ_{max}, which subsequently cause greater lateral displacement damage. Therefore, when the soil is subjected to a ground motion with a longer significant duration, the soil nonlinearity is greater than that of the shorter duration, specifically at higher soil profile thicknesses.

In this study, a homogeneous liquefiable soil profile was considered for conducting the nonlinear liquefaction analysis. Since the real soil profile in the field is multi-layered and inhomogeneous, the influence of ground-motion

characteristics on the seismic behavior of the liquefiable soil could be different from the results given by this study. Despite a number of limitations, the results obtained within this study provide a baseline for demonstrating the seismic behavior of homogeneous liquefiable soil under different ground motion characteristics. Further investigations are required by detailed numerical analyses for the better understanding of the effects of ground motion characteristics on liquefiable soils considering different soil profile variations.

As emphasized in this study, soil nonlinearity causes significant attenuation of ground surface accelerations for the liquefiable soil profile under strong input motions. This phenomenon may be seen favorable for the seismic design of structures, but the shear strains and displacements are amplified pronouncedly concurrently. In practice, such behavior should be carefully handled by engineers in the seismic resistant design of new structures or seismic requalification of existing structures located in areas susceptible to liquefaction.

References

[1] Ishihara, K., Koga, Y. "Case studies of liquefaction in the 1964 Niigata earthquake", Soils and Foundations, 21(3), pp. 35–52, 1981. https://doi.org/10.3208/sandf1972.21.3_35

[2] Shengcong, F., Tatsuoka, F. "Soil liquefaction during Haicheng and Tangshan earthquake in China; A review", Soils and Foundations, 24(4), pp. 11–29, 1984. https://doi.org/10.3208/sandf1972.24.4_11

[3] Youd, T. L. "Geologic effects-liquefaction and associated ground failure", In: Proceedings of the Geologic and Hydraulic Hazards Training Program, Denver, CO, USA, 1984, pp. 210–232.

[4] Yoshida, N., Tokimatsu, K., Yasuda, S., Kokusho, T., Okimura, T. "Geotechnical aspects of damage in Adapazari city during 1999 Kocaeli, Turkey earthquake", Soils and Foundations, 41(4), pp. 25–45, 2001. https://doi.org/10.3208/sandf.41.4_25

[5] Cubrinovski, M., Bray, J. D., Taylor, M., Giorgini, S., Bradley, B., Wotherspoon, L., Zupan, J. "Soil liquefaction effects in the central business district during the February 2011 Christchurch earthquake", Seismological Research Letters, 82(6), pp. 893–904, 2011. https://doi.org/10.1785/gssrl.82.6.893

[6] Yamaguchi, A., Mori, T., Kazama, M., Yoshida, N. "Liquefaction in Tohoku district during the 2011 off the Pacific Coast of Tohoku Earthquake", Soils and Foundations, 52(5), pp. 811–829, 2012. https://doi.org/10.1016/j.sandf.2012.11.005

[7] Youd, T. "Ground Failure Investigations Following the 1964 Alaska Earthquake", presented at Proceedings of the 10th National Conference in Earthquake Engineering, Anchorage, Alaska, July, 21–25, 2014. https://doi.org/10.4231/D3DN3ZW6P

[8] Zeghal, M., Elgamal, A.-W. "Analysis of site liquefaction using earthquake records", Journal of Geotechnical Engineering, 120(6), pp. 996–1017, 1994. https://doi.org/10.1061/(ASCE)0733-9410(1994)120:6(996)

[9] Zorapapel, G. T., Vucetic, M. "The effects of seismic pore water pressure on ground surface motion", Earthquake Spectra, 10(2), pp. 403–438, 1994. https://doi.org/10.1193/1.1585780

[10] Elgamal, A.-W., Zeghal, M., Parra, E. "Liquefaction of reclaimed island in Kobe, Japan", Journal of Geotechnical Engineering, 122(1) pp. 39–49, 1996. https://doi.org/10.1061/(ASCE)0733-9410(1996)122:1(39)

[11] Youd, T. L., Carter, B. L. "Influence of soil softening and liquefaction on spectral acceleration", Journal of Geotechnical and Geoenvironmental Engineering, 131(7), pp. 811–825, 2005. https://doi.org/10.1061/(ASCE)1090-0241(2005)131:7(811)

[12] Bán, Z., Győri, E., Tóth, L., Gráczer, Z., Mahler, A. "Characterization and Liquefaction Hazard Assessment of Two Hungarian Liquefied Sites from the 1956 Dunaharaszti Earthquake", Periodica Polytechnica Civil Engineering, 64(3), pp. 713–721, 2020. https://doi.org/10.3311/PPci.15607

[13] Gingery, J. R., Elgamal, A., Bray, J. D. "Response spectra at liquefaction sites during shallow crustal earthquakes", Earthquake Spectra, 31(4), pp. 2325–2349, 2015. https://doi.org/10.1193/101813EQS272M

[14] Adalier, K., Elgamal, A. "Liquefaction of over-consolidated sand: a centrifuge investigation", Journal of Earthquake Engineering, 9(spec1), pp. 127–150, 2005. https://doi.org/10.1142/S1363246905002195

[15] Su, D., Ming, H. Y., Li, X. S. "Effect of shaking strength on the seismic response of liquefiable level ground", Engineering Geology, 166, pp. 262–271, 2013. https://doi.org/10.1016/j.enggeo.2013.09.013

[16] Adampira, M., Derakhshandi, M., Ghalandarzadeh, A. "Experimental study on seismic response characteristics of liquefiable soil layers", Journal of Earthquake Engineering, 25(7), pp. 1287–1315, 2021. https://doi.org/10.1080/13632469.2019.1568930

[17] Roesset, J. "Soil amplifcation of earthquakes", In: Numerical Methods in Geotechnical Engineering, McGraw-Hill, 1977, pp. 639–682. ISBN 0070165424

[18] Hartvigsen, A. J. "Influence of pore pressures in liquefiable soils on elastic response spectra", MSc Thesis, University of Washington, 2007.

[19] Kramer, S., Hartvigsen, A., Sideras, S., Ozener, P. "Site response modeling in liquefiable soil deposits", presented at 4th International IASPEI Symposium on Effects of Surface Geology on Seismic Motion, Santa Barbara, CA, USA, Aug. 23–26, 2011.

[20] Montoya-Noguera, S., Lopez-Caballero, F. "Effect of coupling excess pore pressure and deformation on nonlinear seismic soil response", Acta Geotechnica, 11, pp. 191–207, 2016. https://doi.org/10.1007/s11440-014-0355-7

[21] Foerster, E., Modaressi, H. "Nonlinear numerical method for earthquake site response analysis II - case studies", Bulletin of Earthquake Engineering, 5, pp. 325–345, 2007.
https://doi.org/10.1007/s10518-007-9034-5

[22] Markham, C. S., Bray, J. D., Macedo, J., Luque, R. "Evaluating nonlinear effective stress site response analyses using records from the Canterbury earthquake sequence", Soil Dynamics and Earthquake Engineering, 82, pp. 84–98, 2016.
https://doi.org/10.1016/j.soildyn.2015.12.007

[23] Bouckovalas, G. D., Tsiapas, Y. Z., Theocharis, A. I., Chaloulos, Y. K. "Ground response at liquefied sites: seismic isolation or amplification?", Soil Dynamics and Earthquake Engineering, 91, pp. 329–339, 2016.
https://doi.org/10.1016/j.soildyn.2016.09.028

[24] Adampira, M., Derakhshandi, M. "Influence of a layered liquefiable soil on seismic site response using physical modeling and numerical simulation", Engineering Geology, 266, 105462, 2020.
https://doi.org/10.1016/j.enggeo.2019.105462

[25] Adampira, M., Derakhshandi, M., Ghalandarzadeh, A., Koupaei, H. J. "Evaluation of one-dimensional seismic site response due to liquefiable sub-layer", Proceedings of the Institution of Civil Engineers-Geotechnical Engineering, 173(2), pp. 133–152, 2020.
https://doi.org/10.1680/jgeen.18.00248

[26] Kuhlemeyer, R. L., Lysmer, J. "Finite element method accuracy for wave propagation problems", Journal of the Soil Mechanics and Foundations Division, 99(5), pp. 421–427, 1973.
https://doi.org/10.1061/JSFEAQ.0001885

[27] Zienkiewicz, O. C., Wood, W. L., Hine, N. W., Taylor, R. L. "A unified set of single step algorithms. Part 1: General formulation and applications", International Journal for Numerical Methods in Engineering, 20(8), pp. 1529–1552, 1984.
https://doi.org/10.1002/nme.1620200814

[28] Yang, Z., Lu, J., Elgamal, A. "OpenSees Soil Models and Solid-Fluid Fully Coupled Elements, User's Manual, 2008 ver 1.0", University of California, San Diego Department of Structural Engineering, San Diego, CA, USA, 2008.

[29] Prevost, J. H. "A simple plasticity theory for frictional cohesionless soils", International Journal of Soil Dynamics and Earthquake Engineering, 4(1) pp. 9–17, 1985.
https://doi.org/10.1016/0261-7277(85)90030-0

[30] Demir, S. "Numerical assessment of the performance of different constitutive models used to predict liquefiable soil behavior", International Advanced Researches and Engineering Journal, 5(2), pp. 260–267, 2021.
https://doi.org/10.35860/iarej.871429

[31] Arulmoli, K., Muraleetharan, K. K., Hossain, M. M., Fruth, L. S. "VELACS: Verification of liquefaction analyses by centrifuge studies, laboratory testing program, Soil data report", The Earth Technology Corporation, Irvine, CA, USA, Project No. 90-0562, 1992.

[32] Kramer, S. L. "Geotechnical Earthquake Engineering", Pearson, 1996. ISBN-10: 0133749436

[33] Kokusho, T. "Seismic base-isolation mechanism in liquefied sand in terms of energy", Soil Dynamics and Earthquake Engineering, 63, pp. 92–97, 2014.
https://doi.org/10.1016/j.soildyn.2014.03.015

[34] Popescu, R., Prevost, J. H., Deodatis, G. "Effects of spatial variability on soil liquefaction: some design recommendations", Géotechnique, 47(5), pp. 1019–1036, 1997.
https://doi.org/10.1680/geot.1997.47.5.1019

[35] Beresnev, I. A., Wen, K.-L. "Nonlinear soil response - A reality?", Bulletin of the Seismological Society of America, 86(6), pp. 1964–1978, 1996.
https://doi.org/10.1785/BSSA0860061964

[36] Kramer, S. L., Sideras, S. S., Greenfield, M. W. "The timing of liquefaction and its utility in liquefaction hazard evaluation", Soil Dynamics and Earthquake Engineering, 91, pp. 133–146, 2016.
https://doi.org/10.1016/j.soildyn.2016.07.025